



RESEARCH ARTICLE

Anatomy and Morphometry of Major Salivary Glands of Domestic Cats with Relation to their Histological Features

Yara S Abouelela^{1*}, Haithem A Farghali², Zainab Sabry Othman Ahmed³ and Reem RT¹

¹Department of Anatomy and Embryology; ²Department of Surgery, Anesthesiology and Radiology

³Department of Cytology and histology, Faculty of Veterinary Medicine, Cairo University, 12211, Egypt

*Corresponding author: yarasayed89@gmail.com

ARTICLE HISTORY (21-094)

Received: February 24, 2021
Revised: September 20, 2021
Accepted: September 25, 2021
Published online: December 07, 2021

Key words:

Felis catus
Major salivary glands
Sialocoele
Sialography
Surgical anatomy

ABSTRACT

The normal descriptive anatomical and histological studies on feline major salivary glands were estimated. We were focusing on clinically valuable glands; parotid, mandibular and sublingual salivary glands, and their ductal pathways by making sialography and papillary cannulation, that can help surgeons in their surgical approach. The work was carried out on seven cadaver domestic cats of both sexes. Anatomical dissection was performed to separate each gland and its duct. A novel papillary cannulation technique was achieved along with the radiographical study which occurred by injecting the ductal papillae with lead oxide dissolved in turpentine oil. Our findings asserted that the parotid gland was caudal to the mandible with a serous secretory unit. Its papilla was located dorsally in the upper buccal mucosa with a curved bent to prevent its occlusion with food particles. Thus, sialocoele was rarely seen in the parotid gland. The mandibular and sublingual salivary glands were closely connected in one compact membrane that has both serous and mucous endpieces. Their ducts passed together in the intermandibular space till they opened in the sublingual caruncles that are easily obstructed by food remnants. Therefore, they are more susceptible to sialocoele. The zygomatic gland was the deepest, while the molar gland appeared at the mandibular lip, which is composed mainly of mucous adenomeres. Eventually, we could provide in the current study a complete descriptive atlas of the major salivary glands of domestic cats, and we explained why sialocoele occurs more frequently in mandibulo-sublingual glands than in parotid glands.

To Cite This Article: Abouelela YS, Farghali HA, Ahmed ZSO and Reem RT, 2022. Anatomy and morphometry of major salivary glands of domestic cats with relation to their histological features. Pak Vet J, 42(1): 81-87. <http://dx.doi.org/10.29261/pakvetj/2021.079>

INTRODUCTION

Feline anatomy was neglected in the anatomical veterinary literatures, as most studies focused on the dog as a Carnivora representative. Salivary glands release saliva which is extensively used in food mastication (Mohammadpour, 2010; EL-Kordy *et al.*, 2014). The major salivary glands of herbivores are more developed than those of carnivores (Mazzullo *et al.*, 2005). The feline major salivary glands include parotid, submandibular, sublingual, zygomatic and molar glands (Tsioli *et al.*, 2015; Fromme *et al.*, 2016; Bassanino *et al.*, 2019). The molar gland is absent in dogs (Adams, 2004; Gaber *et al.*, 2020). The anatomical position of the salivary glands and their ductal pathway have been studied by Gaber *et al.* (2020) in dogs and by Kim *et al.* (2008) in cats and dogs, which helps the surgeons in their

surgical approach (Durand *et al.*, 2016; Shivaraju *et al.*, 2018) and improves the feline oral pain management (Du Toit and Nortje, 2004). As well as, contrast X-rays offer complementary data in cats (Kim *et al.*, 2008) and camel (Rezk and Shaker, 2017). Cannulation of parotid, mandibular and sublingual salivary glands have not been performed on cats up till now, while parotid cannulation was performed on dogs (Dyce *et al.*, 2010). Different clinical conditions affect the salivary glands, as salivary sialoceles, extravasated saliva (Bassanino *et al.*, 2019) and salivary gland neoplasia which is considered the most common affection of the salivary glands, especially in the sublingual one (Kazemi *et al.*, 2012; Bassanino *et al.*, 2019). Sialocoeles are rare in cats than in dogs (Tsioli *et al.*, 2015; Shivaraju *et al.*, 2018) and the most accurate technical diagnosis for sialocoeles is sialography (Bassanino *et al.*, 2019). Thus, in the current study, we

intended to dissect each gland separately with its morphometric parameters. We also focused on the way to perform ductal pathway cannulation through its oral papillae, which helps in saliva aspiration for biochemical evaluation or drug injection through it. We confirmed the proper site to cannulate by sialography technique. Additionally, the normal histological structure of salivary glands including the parenchymatic secretory units was observed to reach a complete descriptive atlas on feline salivary glands.

MATERIALS AND METHODS

Seven feline cadavers of both sexes, with an age range within 2-3 years were used in this study. Cats selected from our Faculty's Hospital in Cairo University after exposure to accidents but with healthy normal heads, we took their history from their owners. Specimens were collected from both sides of the head of each cat. Thus, the current study was carried out on 14 specimens from each gland. Subsequently, the anatomical dissection, sialography technique, ductal cannulation, histological studies were performed immediately within the first 30 minutes after death. Heads that are used for cannulation and sialography must be fresh, non-formalized that allow the oral cavity mucosa to remain soft and received any injectable substances. So, we can store these specimens in a refrigerator during the study.

Anatomical study: Three cats were used for anatomical dissection by removal of the skin and exposure of the glands with their ductal system from both sides. For accurate differentiation between the mandibular and sublingual salivary glands, their sublingual caruncles were injected using gum milk latex coloured with green Rotring® ink. For reaching the zygomatic gland, deep dissection in the head was made by removing the masseter muscle and cutting the zygomatic arch just under the eyeball (Gaber *et al.*, 2020).

Salivary papillae cannulation: Cannulation of the most exposed salivary glands to affections as parotid, mandibular and sublingual was performed for the first time, while molar and zygomatic showed very narrow ducts. For cannulation of the ductal papillae through the oral cavity, the parotid papilla was cannulated by inserting the cannulate in the upper buccal mucosa against the upper second cheek teeth in papilla salivalis (Dyce *et al.*, 2010), while we inserted the cannulate in sublingual space within the sublingual caruncle (Kneissl *et al.*, 2011) to reach the papillae of mandibular and sublingual glands. There were some precautions in cannulation, as the oral mucosa must be grasped to remove the bent in the parotid ductal pathway (Dyce *et al.*, 2010), as well as all papillae must be cannulated in a rotating manner to avoid rupture or penetration of the duct.

Sialography. Radiographic contrast X-ray films were achieved by using a radiographic device (Fisher imaging, Chicago, USA) to recognize the glands normal size, location and ductal systems. Two fresh cadaver cat's heads were injected with lead oxide mixed with turpentine oil and injected into the papillae at the oral cavity using a

very fine needle. The radiographic positions were ventrodorsal and lateral views (Rezk and Shaker, 2017).

Histology: The salivary glands specimens from both sides of two cats were fixed immediately after death within 30 min in 10% neutral buffered formalin, then were processed, and 3-5µm paraffin sections were prepared by the microtome and stained (Bancroft and Gamble, 20082). Harris haematoxylin and eosin stain for general histological studies, Masson's trichrome stain for detection of collagen fibers and Periodic acid-Schiff (PAS) stain for detection of neutral mucopolysaccharides were used. The stained sections were examined by light microscopy (LEICA DM500), then images were captured with the camera (LEICA ICC50 HD) attached to the microscope and eventually examined by the image analysis software.

Statistical analysis: The measurements of the salivary glands were taken on each isolated gland using Vernier Caliber. As the salivary glands had irregular dimensions, we stabilized each salivary gland to take the standardized readings in its width at the widest line and for length estimation at the highest point in each salivary gland. All data was added to a Microsoft Excel sheet, and the results were shown as mean ± SE using SPSS® program version 16, USA (Levesque, 2007).

RESULTS

Parotid salivary gland: Anatomically, the parotid gland is considered the main large one in cats. In the current study, the parotid gland appeared as a triangular flat lobulated gland (Fig. 1A-D), with length 3.53±0.08cm, and width 3.2±0.05cm (Table 1). It rested below the auricular cartilage. Its anterior border covered the posterior border of the masseter muscle, while ventrally it overlapped the dorsal border of the mandibular gland (Fig. 1C) as well as, its caudal border was related to the wing of the atlas.

Parotid ducts (Fig. 1B & C) arose as united several small ducts from the cranioventral angle of the gland (Fig. 1C & D) and passed rostrally parallel to the two terminal branches of the facial nerve in the lateral facial fascia over the masseter muscle which appeared radiographically (Fig. 1B). After that, it was merged through the oral mucosa with a bent twisted portion and perforated the oral vestibule against the upper second cheek teeth as a parotid papilla (Fig. 1E). This papilla is easy to be cannulated through the oral cavity (Fig. 1F).

Histologically, H & E- stained sections of the parotid gland (Fig. 2A-C) exhibited a compound acinar gland that was surrounded by a capsule, from which connective tissue septa extended to divide the gland into lobules. The lobules were formed entirely of densely packed serous acini. Serous acini appeared with basophilic basal cytoplasm and basal spherical nuclei. Intercalated ducts (ICD) and striated ducts (SD) were also seen inside the lobules. ICD was lined by low cuboidal epithelium, while SD was formed of low columnar epithelium that was characterized by very faint pink striation extending from the base of the secretory cells to the level of their nuclei. The interlobular ducts appeared with pseudostratified or

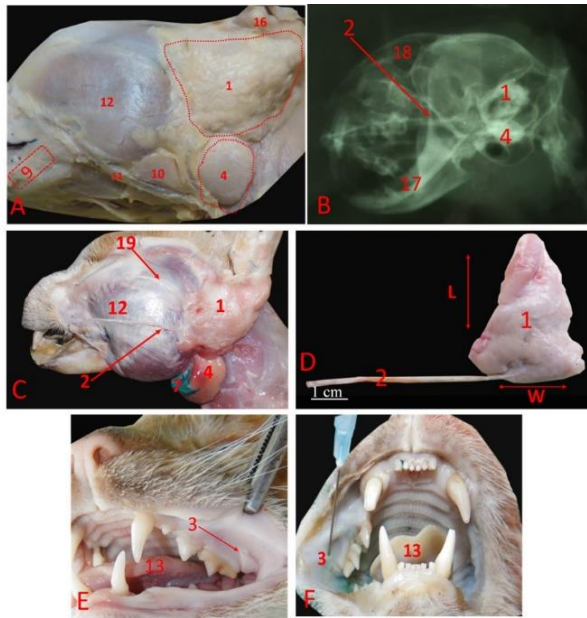


Fig. 1: Anatomy and radiography of feline major salivary glands. **A;** Superficial lateral view of the head, **B;** Lateral radiographic view of the cat head. **C;** lateral view of the cat head after removal of mandibular lymph node, **D;** Separated parotid salivary gland, **E;** Site of Parotid papilla of parotid gland, **F;** Cannulation of parotid papilla in the oral vestibule.

Table 1: The anatomical measuring parameters of healthy cat major salivary glands

Gland	Length (cm)	Width (cm)
Parotid	3.53±0.08	3.20±0.05
Mandibular	2.50±0.05	1.40±0.05
Sublingual	1.23±0.08	3.13±0.08
Zygomatic	1.00±0.11	1.96±0.08
Molar	0.36±0.08	2.03±0.08

stratified columnar epithelium lining. The serous acini were surrounded by myoepithelial cells that were present between the secretory cells and the basal lamina and appeared as spindle-shaped cells. Masson's trichrome stain (Fig. 2D & E) showed blue connective tissue capsule and septa that were observed surrounding the interlobular ducts, thin intralobular connective tissue elements were

also seen between the secretory units. PAS stained sections of the parotid gland (Fig. 2F) revealed a positive reaction of the secretory units that appeared with magenta colour, while the ducts of the parotid gland showed negative reaction and appeared faintly stained with blue nuclei.

Mandibular & Sublingual salivary glands:

Anatomically, the mandibular salivary gland (Fig. 3) appeared symmetrically spherical thick smooth compact, on both sides under the subcutaneous fascia directly, with length 2.5 ± 0.05 cm, and width 1.4 ± 0.05 cm (Table 1). On the other hand, the sublingual gland was elliptical thin gland with length 1.23 ± 0.08 cm, and width 3.1 ± 0.08 cm (Table 1). It seemed like a continuation of the mandibular gland as it lodged on the medial surface of the mandibular one (Fig. 3A, B & C). Mandibular and sublingual were placed in the same capsule ventral to the parotid gland at the caudoventral border of the masseter muscle and rostral to the muscles of the neck. The mandibular lymph nodes were located rostroventral to the mandibular salivary gland, so it covered the sublingual salivary gland (Fig. 1A). The maxillary vein covered the rostral border of the mandibular gland, while the linguofacial veins passed over the mandibular lymph nodes (Fig. 1A).

Mandibular and Sublingual ducts (Fig. 3B, D & E) run rostrally parallel to the medial aspect of the mandibular body in relation to the digastric muscle, lingual muscles ventrally and the medial pterygoid dorsally between the ramus of the mandible and the tongue till they opened in sublingual caruncles which were located caudal to the lower incisor teeth (Fig. 3E). The mandibular duct was erupted at the lateral side of the caruncles, while the duct of the sublingual opened at the medial side of it in a common papilla (Fig. 4A & C). However, two papillae were observed in some cats on the sub-lingual floor; rostral for the opening of the mandibular duct and caudal one for the opening of the sublingual duct (Fig. 4B & C). Depending on the position of these papillae in the sublingual floor made it easily obstructed by remnant food particles and blocked its ductal system.

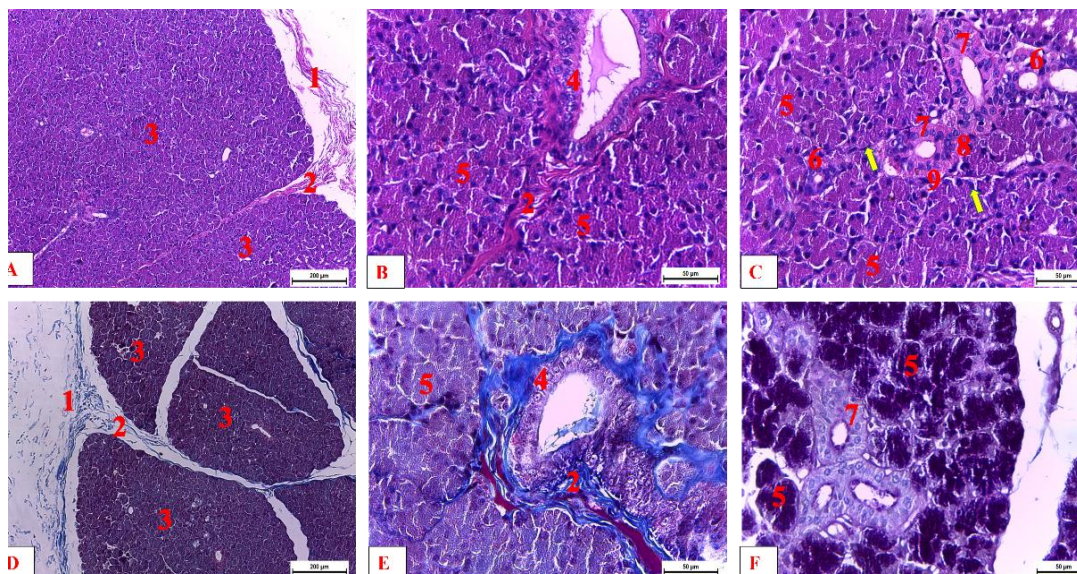


Fig. 2: Histological pictures of feline parotid salivary gland. A (100X) and B & C (400X); H & E-stained sections, D (100X) & E (400X); Masson's trichrome stained sections, F (400X); PAS-stained section.

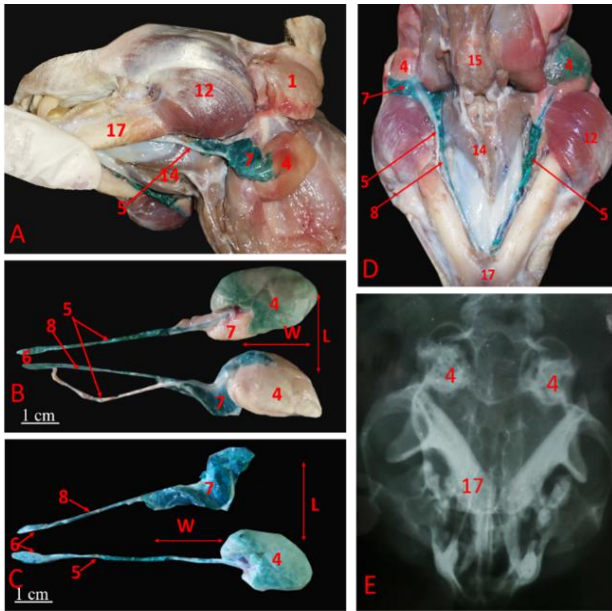


Fig. 3: Anatomy and radiography of feline mandibular and sublingual salivary gland. **A;** Lateroventral view of the head, **B & C;** Separated mandibular and sublingual glands and their ducts, **D;** Ventral view of the head with reflection of omohyoid and anterior digastric muscles **E;** Ventro-dorsal radiographic view of the head.

Histologically, the mandibular gland was a compound tubuloacinar gland with a thin connective tissue capsule with serous acini and mucous tubules. Serous demilune was also seen. Myoepithelial cells were detected between the basal lamina and the secretory cells. The duct system inside the lobule was obtained formed of intercalated ducts, striated ducts and interlobular ducts (Fig. 5A, B & C). Masson's trichrome stain showed the blue stained capsule and septa, in addition to the thin supporting connective tissue between the secretory units (Fig. 5D & E). PAS stained sections exhibited a strong positive reaction of the mucous secretory cells that appeared with deep magenta colour, while the serous secreting cells appeared with lighter magenta colour. The duct system showed a negative reaction to PAS stain and appeared faintly stained (Fig. 5F). On the other hand, the sublingual salivary gland revealed a compound tubuloacinar gland that had a scant connective tissue capsule that sent septa to divide the gland into lobes and lobules. The lobules were composed of serous and mucous secretory units, but the serous acini predominated. Adipocytes were also observed in the gland parenchyma. Intercalated ducts, striated ducts and interlobular ducts were also seen (Fig. 5G, H & I). Masson's trichrome stain showed blue-stained

connective tissue capsule and septa (Fig. 5J & K), while PAS stain exhibited deep magenta colour of mucous secretory units and light magenta colour of the predominated serous acini (Fig. 5L).

Zygomatic salivary gland: Anatomically, the Zygomatic salivary gland (Fig. 6A & B) was the only deep one in the feline major salivary glands. It was pyramidal compacted and glandular with apex directed ventrally and base directed dorsally. Its length was recorded 1 ± 0.11 cm, and width 1.96 ± 0.08 cm (Table 1). Its dorsal border was related to the periorbital fat, while the dorsomedial one was correlated to the eyeball, so it is called the infraorbital gland. Laterally, it is covered by the zygomatic arch. Its posterior border was related to the ramus of the mandible, while its rostral border was near the maxillary lip. All previously mentioned boundaries were hidden by the masseter muscle. Its duct was short and narrow which arose from the ventral border of the gland, so its cannulation was very difficult.

Histologically, the zygomatic gland exhibited dense irregular connective tissue capsule and composed of serous and mucous secretory units, but the mucous adenomeres predominated. The secretory units were surrounded by myoepithelial cells. The intercalated duct appeared large with the wide lumen and lined with cuboidal epithelium (Fig. 7A-C). Masson's trichrome stain showed thin connective tissue capsule and septa, in addition to the scant intralobular connective tissue (Fig. 7D & E). The intercalated duct appeared large with a wide lumen (Fig. 7F). PAS stained sections revealed a strong positive reaction of the mucous adenomeres that appeared as deep magenta colour (Fig. 7G).

Molar salivary gland: Molar salivary gland (Fig. 6C & D) was quadrilateral elongated granular in shape with yellowish colouration with length 0.36 ± 0.08 cm, and width 2.03 ± 0.08 cm (Table 1). It appeared in the submucosal fascia of the lower lip related to the orbicularis oris muscle in the vicinity of the oral commissure just rostral to the masseter muscle, while the facial vein overlapped the caudal border of the gland and has several small ducts drained into the oral vestibule.

Histologically, the molar gland appeared compound tubuloalveolar gland, which was composed mainly of secretory long branched mucous tubules, with a small number of serous acini and serous demilunes. Intercalated ducts and striated ducts were not seen, while the interlobular ducts appeared having 2 layers of cuboidal cells (Fig. 7H-J). With Masson's trichrome stain, collagen

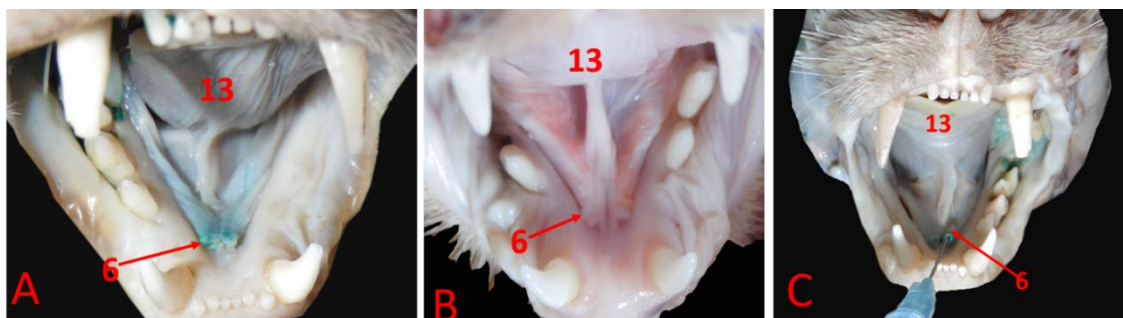


Fig. 4: Anatomy of feline sublingual floor. **A & B;** the latex injected and fresh sublingual caruncle respectively, **C;** Cannulation of the sublingual caruncle.

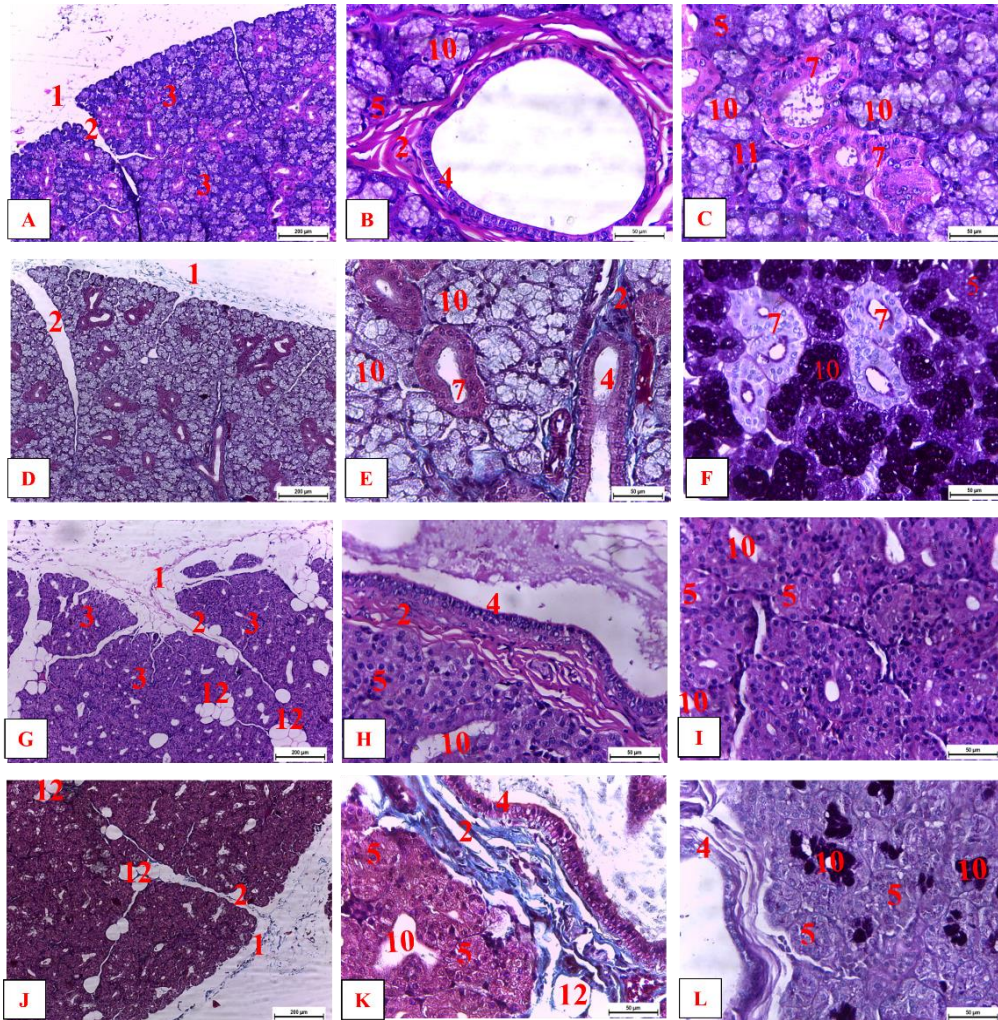


Fig. 5: Histological pictures of feline mandibular and sublingual salivary glands. **A-F** photomicrographs resemble the mandibular gland. **A** (100X) and **B & C** (400X); H&E-stained sections, **D** (100X) & **E** (400X); Masson's trichrome stained sections, **F** (400X); PAS-stained section. **G- L** photomicrographs represent the sublingual gland. **G** (100X) and **H & I** (400X); H&E-stained sections, **J** (100X) & **K** (400X); Masson's trichrome stained sections, **L** (400X); PAS-stained section.

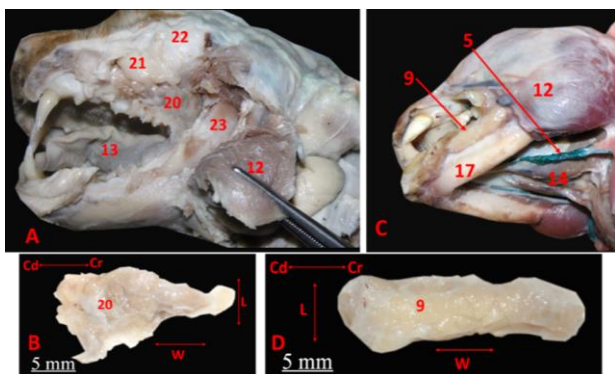


Fig. 6: Anatomy of feline zygomatic and molar salivary gland. **A**; Lateral deep view of head after reflection of masseter muscle, **B**; Separated zygomatic salivary gland, **C**; Lateroventral view of head, **D**; Separated molar salivary gland.

Legend of Figures (1, 3, 4 & 6): 1. Parotid salivary gland, 2. Duct of parotid salivary gland, 3. Papilla salivaris, 4. Mandibular salivary gland, 5. Duct of mandibular salivary gland, 6. Sublingual caruncle, 7. Sublingual salivary gland, 8. Duct of sublingual salivary gland, 9. Molar salivary gland, 10. Mandibular lymph node, 11. Facial vein, 12. Masseter muscle, 13. Tongue, 14. Genioglossus muscle, 15. Omohyoids and anterior digastric muscles, 16. Auricular cartilage, 17. Mandibula, 18. Frontal sinus, 19. Dorsal buccal nerve, 20. Zygomatic salivary gland, 21. Periocular fat, 22. Eye ball, 23. Ramus of the mandible.

fibers appeared with a bluish colouration of the stained capsule, septa and the intralobular connective tissue around the secretory units, while the nuclei appeared black (Fig. 7K & L). PAS-stained sections revealed the deep magenta colour of the mucous secretory cells, indicating the strong positive reaction of the secretory cells against the faint-stained background (Fig. 7M).

DISCUSSION

Our results revealed that the feline major salivary glands included parotid, mandibular, as well as sublingual glands like that of herbivores including rabbits (Matosz *et al.*, 2018). Moreover, the zygomatic salivary gland was also appeared and represented the dorsal buccal glands as in dogs (Kneissl *et al.*, 2011; Mohamed, 2020), in fox (Pereira and Faria Júnior, 2018), as well as in roe deers (Mohammadpour, 2009). Moreover, a special appearance of the molar salivary gland was noticed. It is considered a union of buccal glands in cats only (Mohammadpour, 2010; Mohammadpour, 2011). On the other hand, Mohammadpour (2009) reported that the molar gland is present in ferrets too.

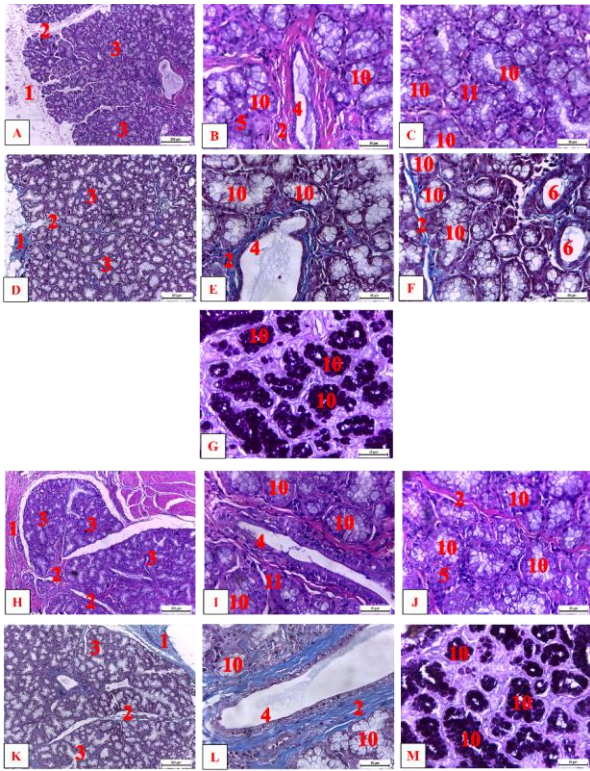


Fig. 7: Histological pictures of feline zygomatic and molar salivary glands. **A-G:** Stained sections of zygomatic gland. **A** (100X) and **B & C** (400X); H& E-stained sections, **D** (100X) and **E & F** (400X); Masson's trichrome stained sections, **G** (400X); PAS-stained section. **H-M:** Stained sections of molar gland. **H** (100X) and **I & J** (400X); H& E-stained sections, **K** (100X) and **L** (400X); Masson's trichrome stained sections, **M** (400X); PAS-stained section.

Legend of Figures (2, 5, & 7): 1.capsule, 2. Septa, 3. Lobule, 4. Interlobular duct, 5. Serous acini, 6. Intercalated duct, 7. Striated duct, 8. Striation, 9. Myoepithelial cells, 10. Mucous secretory unit, 11. Serous demilune. 12. Adipocytes.

The most advanced salivary gland in the cat was the parotid gland as in horse, swine, and dog which is against that already reported by EL-Kordy *et al.* (2014). On other hand, the mandibular was the main one in the cow. The parotid gland was triangular and situated caudal to the masseter muscle that resembles in crab-eating-fox (Pereira and Faria Júnior, 2018), while Matosz *et al.* (2018) believed that the parotid gland elongated as it reached the mandibular angle in rabbit. Likewise, Hussein (2016), in rabbit, also confirmed that it placed on either side of trachea underneath the larynx, although in camel, it was reported that it was rectangular in its outline (Rezk and Shaker, 2017). Our findings showed the purely serous secretory cells in the parotid gland and the mixed nature in the other four glands which are nearly similar to the results of Khosravani *et al.* (2007) in ferrets.

In our study, parotid duct run over the masseter muscle to open through the parotid papilla against the upper second cheek teeth in cat oral vestibule which is in line with what was reported by Dyce *et al.* (2010), while it opens in dogs at the last cheek teeth (Adams, 2004). However, Dyce *et al.* (2010) and Kneissl *et al.* (2011) added that it opens in dogs against the third or the fourth premolar upper tooth. In rabbits, it perforated at the last superior molar (Hussein, 2016; Matosz *et al.*, 2018), while it opened at the level of the 4th molar tooth superiorly in

camel (Rezk and Shaker, 2017). The parotid papilla was located dorsally in the upper buccal mucosa with a curved bent that prevents its occlusion with food particles, so sialocoeles were rare in it.

Cannulation of the parotid salivary gland was performed previously on dogs (Dyce *et al.*, 2010) but not on cats, while cannulation of mandibular and sublingual ducts through its sublingual caruncles has not been recognized up till now even in dogs.

The mandibular gland was compact and lodged within a firm fibrous coat, so it was easily palpable and floated under investigating fingers (Dyce *et al.*, 2010; Kazemi *et al.*, 2012). In the current study, the mandibular gland is placed below the parotid salivary gland. This finding comes in the same line with what was reported in dogs (Kazemi *et al.*, 2012) and minipig (Zhang *et al.*, 2005), while it was lodged in the atlantal fossa and reached to basiohyoid bone in crab-eating-fox (Pereira and Faria Júnior, 2018). On the other hand, Matosz *et al.* (2018) stated that it is located in intermandibular space on both sides of the aboral angles of the tongue in rabbits. In cats of the current study, the gland was round in its outline, undivided and symmetric on both sides. These results agreed with what was reported in dogs by Weidner *et al.* (2012). In minipig, Zhang *et al.* (2005) reported that the mandibular gland was pear in shape. Moreover, it was noticed anterior to the retropharyngeal lymph node in the terrier dog breed (Durand *et al.*, 2016). The mandibular salivary gland in the current study exhibited both mucous and serous secretory units, in contrast to what was recorded by Khosravani *et al.* (2007) who mentioned that the mandibular gland has mainly serous acini. Moreover, the cat sublingual gland is smaller than that of dogs (Tsioli *et al.*, 2015), while it was located in the occipitomandibular region in crab-eating-fox (Pereira and Faria Júnior, 2018). It was also noticed just under the root of the tongue in rabbits (Al-Saffar and Simawy, 2014). The serous acini predominated in sublingual gland in the current study, which was against the findings of Khosravani *et al.* (2007).

Ducts of both mandibular and sublingual glands were passed in the same manner till they penetrated the sublingual floor at their caruncles. These caruncles were more susceptible to sialocoele because of the accumulation of food particles in them. Thus, the ducts of the mandibular and sublingual glands were occluded that preventing the saliva release, leading to accumulation of it and forming sialocoele. Both ducts were easily cannulated, this was unlike what was documented by Dyce *et al.* (2010) who proposed that the mandibular duct was easily cannulated than the sublingual one.

The zygomatic salivary gland was located ventral to the lateral canthus of the eye as was reported by Mohammadpour (2009) and Fromme *et al.* (2016) in cats and by Mohamed (2020) in dogs. Thus, the swelling of the zygomatic salivary gland (zygomatic mucocele) in cats could make a protrusion of the eyeball (exophthalmus) (Dyce *et al.*, 2010). Moreover, Durand *et al.* (2016) in dog asserted that it may take an atypical situation at the ventrorostral border of the masseter muscle beneath the skin (Kneissl *et al.*, 2011). Regarding the zygomatic intercalated duct, it was present with a wide lumen and lined by cuboidal epithelium. These findings

are consistent with what was reported in the dog zygomatic gland (Gaber *et al.*, 2020; Mohamed, 2020). On the other side, our findings disagreed with what was reported in ferrets by Mohammadpour (2010).

The molar salivary gland is located in the inferior lip in a domestic cat, while it is absent in dogs (Adams 2004; Bassanino *et al.*, 2019; Gaber *et al.*, 2020). In our study, it appeared rectangular in shape and placed caudally in front of the facial vein. This finding is consistent with what was described by Mohammadpour (2009) and by Mohammadpour (2011). However, we disagreed with the results of the study performed by Mohammadpour (2010) who stated that it appeared rostrally to the transverse jugular vein. Regarding the molar gland of cats, we found that it was formed mainly of mucous tubules that reacted strongly positive to PAS stain and appeared dark magenta, with an absence of the intercalated and striated duct, which comes in the same line with what was observed by Mohammadpour (2011).

Conclusions: Our work discussed in detail the major salivary glands in the domestic cat. We focused on several aspects as their normal anatomical features and morphometric parameters. We also narrated the ductal papillary cannulation that is a novel studying aspect in domestic cats, as sialography is one of the most important diagnostic technique for any occlusion in a salivary pathway. We also performed a histological study on each gland. Eventually, we can give a complete picture of the normal feline major salivary glands that can be used as a reference against any pathological and surgical conditions.

Ethical approval: Ethical approval (VET CU24112020254) for this study was provided by Veterinary Medicine Cairo University Institutional Animal Care and Use Committee (Vet- CU- IACUC).

Authors contribution: YSA and RRT performed the anatomical study, gland cannulations and statistical analysis. HAF illustrated the radiological contrast study. ZSOA revealed the histological study. All authors reviewed and approved the last version of the manuscript.

Funding: The authors obtained no particular funding from funding agencies for this work.

REFERENCES

Adams DR, 2004. Canine anatomy, a systemic study Fourth Edition, Iowa State Press.
Al-Saffar FJ and Simawy MSH, 2014. Histomorphological and histochemical study of the major salivary glands of adult local rabbits. *Int J Adv Res* 2:378-402.

Bancroft JD and Gamble M, 2008. Theory and practice of histological techniques. Elsevier Health Sciences.
Bassanino J, Palierne S, Blondel M, *et al.*, 2019. Sublingual sialoceles in a cat. *J Feline Med Surg Open Reports* 5:2055116919833249.
Durand A, Finck M, Sullivan M, *et al.*, 2016. Computed tomography and magnetic resonance diagnosis of variations in the anatomical location of the major salivary glands in 1680 dogs and 187 cats. *Vet J* 209:156-62.
Dyce KM, Sack WO and Wensing CJG, 2010. Textbook Of Veterinary Anatomy, By Saunders, An Imprint of Elsevier Inc.
EL-Kordy EA, Alanazi AD, Ali SS, *et al.*, 2014. Histological, histochemical and ultrastructural changes in the submandibular gland of starved young male cats. *J Cytol Histol* 5:252-60.
Fromme V, Köhler C, Piesnack S, *et al.*, 2016. Computed tomographic anatomy of the salivary glands in the cat. *Tierarztl Prax Ausg K Kleintiere Heimtiere* 44:16-25
Gaber W, Shalaan SA, Misk NA, *et al.*, 2020. Surgical anatomy, morphometry, and histochemistry of major salivary glands in dogs: Updates and Recommendations. *Int J Vet Health Sci Res* 8:252-9.
Hussein AA, 2016. Comparative morphological and histological study of the parotid salivary gland in rabbit after birth. *Diyala J Pure Sci* 12:14-23.
Kazemi D, Doustar Y and Assadnassab G, 2012. Surgical treatment of a chronically recurring case of cervical mucocele in a German Shepherd Dog. *Case Reports Vet Med: Article ID 954343*, 4.
Khosravani N, Ekman R and Ekström J, 2007. Acetylcholine synthesis, muscarinic receptor subtypes, neuropeptides and secretion of ferret salivary glands with special reference to the zygomatic gland. *Arch Oral Biol* 52:417-26.
Kim H, Nakaichi M, Itamoto K, *et al.* 2008. Malignant mixed tumour in the salivary gland of a cat. *J Vet Sci* 9:331-333.
Kneissl S, Weidner S and Probst A, 2011. CT Sialography in the Dog – A Cadaver Study. *Anat Histol Embryol* 40:397–401.
Levesque R, 2007. Programming and data management: A guide for SPSS and SAS users, fourth Edition, Chicago, USA.
Matosz B, Dezdrobotu C, Martonos C, *et al.*, 2018. Topography of the major salivary glands in rabbits. *Sci Work Ser C Vet Med* 63:11-4.
Mazzullo G, Sfacteria A, Iannelli N, *et al.*, 2005. Carcinoma of the submandibular salivary glands with multiple metastases in a cat. *Vet Clin Path* 34:61–4.
Mohamed R, 2020. The labial and zygomatic salivary glands in mixed breed dogs in Trinidad: Anatomical location, histological features and histochemical characteristics. *World Vet J* 10:223-30.
Mohammadpour AA, 2009. Investigations on the shape and size of molar and zygomatic salivary glands in shorthair domestic cats. *Bulg J Vet Med* 12:221-5.
Mohammadpour AA, 2010. Anatomical and histological study of molar salivary gland in domestic cat. *Iran J Vet Res* 11:2.
Mohammadpour AA, 2011. Histochemical characteristics of cat molar salivary gland. *Indian Vet J* 88:89-90.
Pereira TSB, and Faria Júnior WH, 2018. Anatomical description of the salivary glands: parotid, mandibular and sublingual of the crab-eating-fox. *Acta Sci Bio Sci* 40:e37528.
Rezk HM and Shaker N, 2017. Parotid and mandibular salivary glands segmentation of the one humped dromedary camel (*Camelus dromedarius*). *Int J Adv Res Bio Sci* 4:32-41.
Shivaraju S, Maiti SK, Kalaiselvan, *et al.*, 2018. Surgical management of cervical mucocele associated with ranula in a dog. *MOJ Anat Physiol* 5:201–3.
Tsioli V, Brellou G, Siziopkou C, *et al.*, 2015. Sialoceles in the cat. A report of 2 cases. *J Hellenic Vet Med SOC* 66:141-6.
Zhang X, Li J, Liu XY, *et al.*, 2005. Morphological characteristics of submandibular glands of miniature pig. *Chin Med J* 118:1368-73.